

The effect of Al(III) and Fe(III) ions on the flotation behavior of K-feldspar with sodium oleate as the collector

Chen Yi ^{1,2}, Jikui Zhou ², Guichun He ¹, Hongxi Hu ², Chao Liu ², Jiping Yang ², Xianjin Lyu ²

¹ Jiangxi Key Laboratory of Mining Engineering, School of Resources and Environmental Engineering, Jiangxi University of Science and Technology, Ganzhou 341000, China

² State Key Laboratory of Rare Metals Separation and Comprehensive Utilization, Institute of Resource Utilization and Rare Earth Development, Guangdong Academy of Sciences, Guangzhou 510650, China

Corresponding author: zhoujk2004@126.com (Jikui Zhou)

Abstract: The present study investigates the effects and mechanisms of aluminum (Al(III)) and iron (Fe(III)) ions on the flotation efficiency of potassium feldspar (K-feldspar) within oleate collector systems. The study employs micro-flotation experiments, solution chemistry calculations, zeta potential measurements, and FT-IR and XPS analyses to demonstrate that Al(III) and Fe(III) ions can significantly improve the flotation recovery of K-feldspar by altering its surface charge, bonding properties, and adsorption modes. The study also develops adsorption models for the flotation of K-feldspar activated by Al(III) and Fe(III), revealing the synergistic impacts of metal ion hydrolysis products and sodium oleate in the formation of hydrophobic complexes.

Keywords: K-feldspar flotation, aluminum ion, iron ion, sodium oleate, action mechanism

1. Introduction

Feldspar, an aluminosilicate mineral abundant in sodium, potassium, and calcium, represents one of the most ubiquitous components of the Earth's crust, constituting over 60% of its total composition. It is extensively distributed in rocks, soils, and other unconsolidated sediments on the Earth's surface and serves as a fundamental constituent of igneous, metamorphic, and sedimentary rocks. From an economic perspective, the majority of feldspar extraction occurs from granites (Heyes et al., 2012; Sanz et al., 2022). Its structure, comprising aluminum, silicon, and oxygen atoms, results in the formation of a stable tetrahedral lattice architecture (Yang et al., 2014).

In the field of mineralogy, K-feldspar, denoted chemically as KAlSi_3O_8 , represents a crucial element of the feldspar mineral group. Its primary applications include the production of high-strength electrical porcelain, ceramics, and durable glass. Compared to other feldspars, K-feldspar is relatively less abundant in industrial uses (Zhang et al., 2018; Gaied and Gallala, 2015). The quality of K-feldspar is largely influenced by its crystalline morphology, presence of impurities affecting its color, and the $\text{K}_2\text{O}/\text{Na}_2\text{O}$ ratio (percentage composition). Flotation, a method known for enhancing feldspar quality, enables the separation of K-feldspar from other minerals, thereby improving its purity and $\text{K}_2\text{O}/\text{Na}_2\text{O}$ ratio (Demir et al., 2004).

Flotation, a physicochemical separation technique, provides significant economic benefits over alternative methods (Heyes et al., 2012). Mainly, research on feldspar flotation examines the operational mechanisms of anionic or cationic collectors and activators during the separation process involving feldspar, quartz, and other minerals. Particularly in anionic collector systems, metallic ions can enhance the collector's adhesion to the mineral surface through precipitation or adsorption, thereby notably improving feldspar mineral flotation (Gao et al., 2021). A detailed investigation of metallic ions' adsorption properties on mineral surfaces enables a precise assessment of their impact on silicate mineral flotation. Simultaneously, the selective activation of silicate minerals by metallic cations relates to the ions' charge. Generally, high-valence metallic ions exert a more significant activating and dispersing influence on minerals compared to their low-valence counterparts (Zhou et al., 2011; Xu et

al., 2018; Kuang et al., 2022). Conducting fundamental research to thoroughly understand the mechanisms of feldspar flotation and verify the influence of metallic ions is therefore essential.

Fourier Transform Infrared Spectroscopy (FT-IR) and X-ray Photoelectron Spectroscopy (XPS) analyses indicate that the flotation of K-feldspar with low concentrations of dodecyl ammonium chloride enhances feldspar floatability through the exchange of K^+ ions with Ba^{2+} ions. Conversely, at higher concentrations, considerable adsorption of Ba^{2+} on the K-feldspar surface causes a notable inhibitory effect (Song et al., 2018). Under natural conditions, the selectivity of sodium feldspar for Ca^{2+} enables a rapid exchange between Na^+ and Ca^{2+} , resulting in substantial calcium adsorption, which increases the surface's positive charge and affects the adsorption of ionic adsorbents (Demir et al., 2003). During the anionic collector flotation of feldspar, both Pb^{2+} and Fe^{3+} ions demonstrate significant activation properties (Gülsoy, n.d.; Jie et al., 2014). Solution chemistry calculations and adsorption measurements reveal that, in the flotation process of sodium feldspar, Fe^{3+} ions bind to the feldspar surface as ferric hydroxide. Moreover, the Fe^{3+} can modify the metallic bond characteristics of the feldspar surface, thereby facilitating the adsorption of sodium oleate (NaOL) onto the mineral surface via its carboxylate groups (Zeng et al., 2022).

Previous research has extensively investigated the roles of Fe^{3+} and Ca^{2+} ions in feldspar flotation, but the role of Al^{3+} has not been sufficiently examined. Al^{3+} possesses a high valence state, providing a unique opportunity to study the activation and dispersion effects of high-valence metal ions on silicate minerals like feldspar. Its unique properties may offer new insights into the flotation mechanisms. Additionally, the interactions between Al^{3+} and other constituents within the flotation system, including NaOL, need further research. Such interactions may result in synergistic effects, potentially improving the flotation efficiency of feldspar. This study employs NaOL as the collector and Fe^{3+} and Al^{3+} as the activators for K-feldspar flotation. It compares the effects of these ions on mineral flotation through micro flotation experiments. Additionally, this study uses zeta potential measurements, FTIR, and XPS to elucidate the adsorption modes and operational mechanisms of Fe^{3+} and Al^{3+} on the mineral surface.

2. Experimental

2.1. Materials and reagents

The K-feldspar ore used in this study was originated from Xinjiang, China. The crude ore was manually crushed and screened, then ground in a ceramic ball mill to obtain two size fractions: $-0.074\text{ mm} \sim +0.038\text{ mm}$ and -0.038 mm . These ore samples were rinsed with ultrapure water three times, then filtered and dried, making them ready for micro-flotation experiments and other analyses. The purity of the ore samples was verified by X-ray diffraction (XRD) spectral analysis, as presented in Fig. 1, and chemical composition analysis, as illustrated in Table 1, which met the experimental requirements.

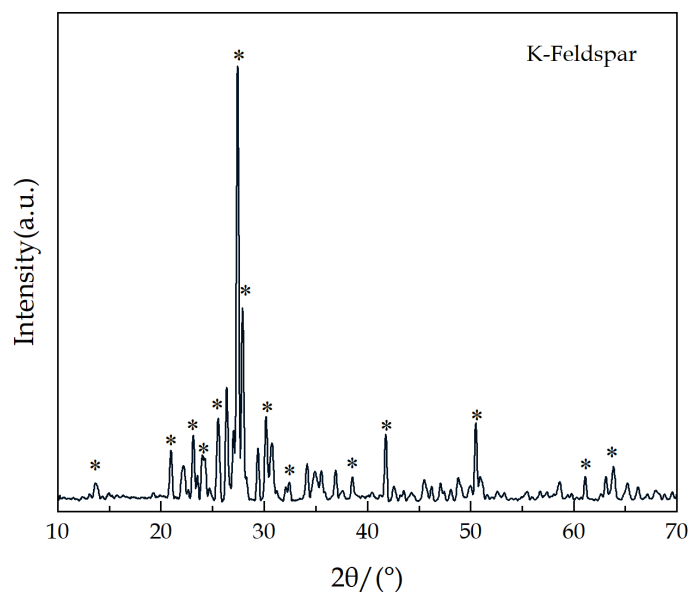


Fig. 1. X-ray diffraction (XRD) spectra of K-feldspar

Table 1. Chemical composition analysis of mineral samples

Minerals	Chemical composition (%)					
	Na ₂ O	K ₂ O	Al ₂ O ₃	SiO ₂	Fe ₂ O ₃	Other
K-feldspar	3.34	12.57	17.87	64.2	0.049	1.971

In this experiment, the flotation reagents utilized were NaOL (96% purity) obtained from Shanghai Macklin Biochemical Co., Ltd.; anhydrous ferric chloride ($\geq 97\%$ purity) and aluminum chloride hexahydrate ($\geq 98\%$ purity) purchased from Sinopharm Chemical Reagent Co., Ltd.; and sodium hydroxide ($\geq 96\%$ purity) and hydrochloric acid (concentration $\geq 36\%$) sourced from Guangzhou Chemical Reagent Factory. NaOL served as the collector, while anhydrous ferric chloride and aluminum chloride hexahydrate acted as activators. Sodium hydroxide and hydrochloric acid were used for pH adjustment. All agents were prepared into solutions before use and the water used in the experiments was ultrapure water with a resistivity of $18.2 \text{ M}\Omega \cdot \text{cm}$.

2.2. Micro-flotation experiments

The single mineral flotation experiment was conducted on an XFG type hanging trough flotation machine with a tank capacity of 40 mL. Each flotation trial involved approximately 2 g of sample, mixed with an appropriate quantity of ultrapure water. The impeller rotation speed was set at 1600 r/min and after one minute of stirring, the pH value of the slurry was adjusted using sodium hydroxide or hydrochloric acid solution, with the adjustment period lasting three minutes. According to experimental requirements, an appropriate amount of activator and collector were sequentially added, each substance stirred for three minutes. The flotation process lasted for two minutes. Concentrate and tailings were separately filtered, dried, and weighed to calculate the flotation recovery rate of the single mineral.

2.3. Zeta-potential measurements

In the initial phase, pure mineral samples were ground to a particle size of $-5 \mu\text{m}$ from an initial size of -0.038 mm . For each test, 50 mg of the sample was introduced into a beaker, filled up to 40 mL with ultrapure water, and subjected to the flotation reagent system. Following this, agitation was instigated using a magnetic stirrer, followed by a 10-minute static placement period. The supernatant was then collected for subsequent measurement. A Zetaplus potential analyzer was used to determine the zeta potential of the mineral surface. Each sample was subjected to three separate measurements, with the final result being the average of these trials.

2.4. FT-IR spectroscopy

For each sample preparation, a 2 g ore sample of -0.038 mm particle size was added into the flotation tank. The sample was processed following the same procedure as in the flotation experiment, with post-reagent treatment filtration performed using microporous filter paper. The filtered ore sample underwent a triple washing process with water at the experiment's pH level, followed by another filtration step. Subsequently, the sample was transported to a vacuum drying oven for drying at 40°C . Upon drying, the resultant sample was subjected to testing using an FT-IR spectrometer.

2.5. XPS experiments

In each test, a 2 g particle size -0.038 mm sample was treated with the same agent used in the micro-flotation experiment, followed by thorough mixing and filtration. Subsequently, the samples were rinsed 2 to 3 times with water, maintaining the same pH as the flotation test, and underwent additional filtration. These filtered specimens were then transferred to a vacuum drying oven and dried at 40°C . Finally, XPS was employed to examine the dried samples.

3. Results and discussion

3.1. Micro-flotation

Fig. 2 illustrates the effect of pH on the flotation recovery of K-feldspar, using 6×10^{-4} mol/L NaOL as a collector, both with and without metal ions. Data analysis reveals a less floatability of K-feldspar when no metal salts are added. This is likely due to the similarity in surface chemical properties between feldspar and quartz, both possessing a point of zero charge (PZC) approximately between 1.5 and 2.5. Consequently, without activating ions, anionic collectors have difficulty to float feldspar (Xu et al., 2017; Fuerstenau and Pradip, 2005). Upon the addition of 2×10^{-4} mol/L of Al^{3+} and Fe^{3+} , the flotation recovery rate of K-feldspar follows an initial increase and subsequent decrease trend as pH rises. Therefore, the presence of Fe^{3+} and Al^{3+} significantly enhances the flotation recovery rate of K-feldspar. Specifically, Fe^{3+} has a considerable effect on the flotation of K-feldspar across a wide pH range, achieving nearly a 90% recovery rate at pH 9. In contrast, Al^{3+} exhibits a more pronounced influence under slightly alkaline conditions, exceeding a recovery rate of 90% at pH 10. The experimental results highlight the remarkable improvement in the flotation performance of K-feldspar due to these two metal ions.

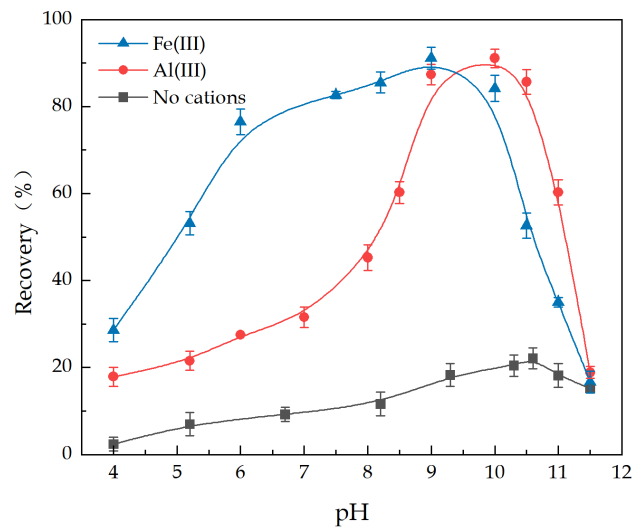


Fig. 2. Effect of pH value on flotation recovery of K-feldspar

Fig. 3 illustrates that upon the introduction of Al^{3+} (at pH 10, with a NaOL dosage of 6×10^{-4} mol/L), the recovery rate of K-feldspar gradually increased as the Al^{3+} concentration increased, provided that the ion concentration remained below 0.8×10^{-4} mol/L. When Al^{3+} concentration ranges within 0.8×10^{-4} to 2×10^{-4} mol/L, K-feldspar maintains a relatively high recovery rate. However, the recovery rate begins to drop as the Al^{3+} concentration increases further. Similarly, when Fe^{3+} was added, the change in K-feldspar's recovery rate follows a trend similar to that observed with Al^{3+} , and sustains a high recovery rate is obtained when the Fe^{3+} concentration is 1.3×10^{-4} mol/L. A sharp decline in the recovery rate occurs when the metal ion concentration becomes excessively high. This could be attributed to the uninteracted metal ions bonding with the collector, thereby reducing the chance of the collector interacting with the mineral surface (Wang et al., 2020).

3.2. Computational analysis of solution chemistry

NaOL, a strong base and weak acid salt, comprises mainly of $\text{RCOOH}(\text{l})$, $\text{RCOOH}(\text{aq})$, RCOO^- , $(\text{RCOO}^-)_2^{2-}$, and RCOOH-RCOO^- in its aqueous solution. Fig. 4 presents a relationship diagram depicting the logarithm of the concentration of each component in the NaOL aqueous solution against pH for an initial concentration of 6×10^{-4} mol/L.

Fig. 4(a) illustrates that under highly acidic conditions, NaOL primarily exists as oleic acid molecules, which hinder its interactions with the minerals. With an increase in the pH level, the concentrations of RCOO^- , $(\text{RCOO}^-)_2^{2-}$, and RCOO^- ions rise correspondingly until reaching pH 8.73. At this point, RCOO^-

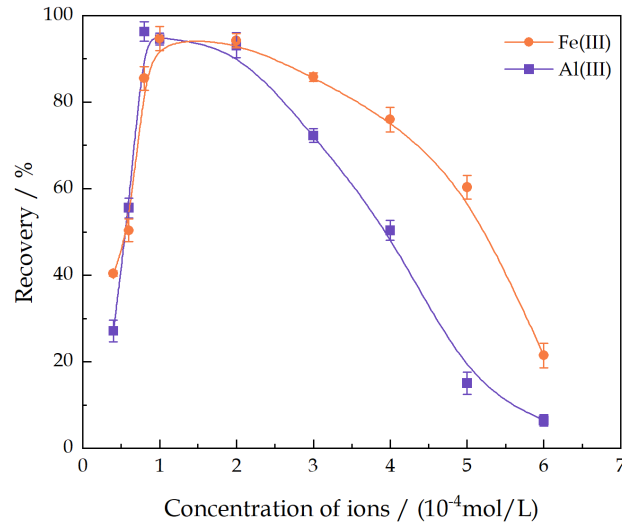


Fig. 3. Effect of metal ion concentration on flotation of K-feldspar (with $6 \times 10^{-4} \text{M}$ NaOL)

and $(\text{RCOO-})_2^{2-}$ become saturated, and the ion-molecule complex concentration of RCOOH-RCOO- reaches its peak. Beyond pH 8.73, the solution predominantly comprises ionic forms, particularly $(\text{RCOO-})_2^{2-}$ and RCOO- . In highly alkaline environments, hydroxyl ions compete with oleate ions for adsorption, thereby influencing the formation of complexes and hindering the collection function of NaOL. This finding is consistent with the flotation results, suggesting that the high recovery phase of K-feldspar flotation corresponds to the pH at which the active components of NaOL, $(\text{RCOO-})_2^{2-}$ and RCOO- , predominantly facilitate the flotation of K-feldspar (Chen et al., 2017; Feng et al., 2018).

Metal ions in the solution undergo hydrolysis, resulting in a diverse array of hydroxy complexes or hydroxide precipitates. The composition ratio of these hydrolysis products varies according to the pH

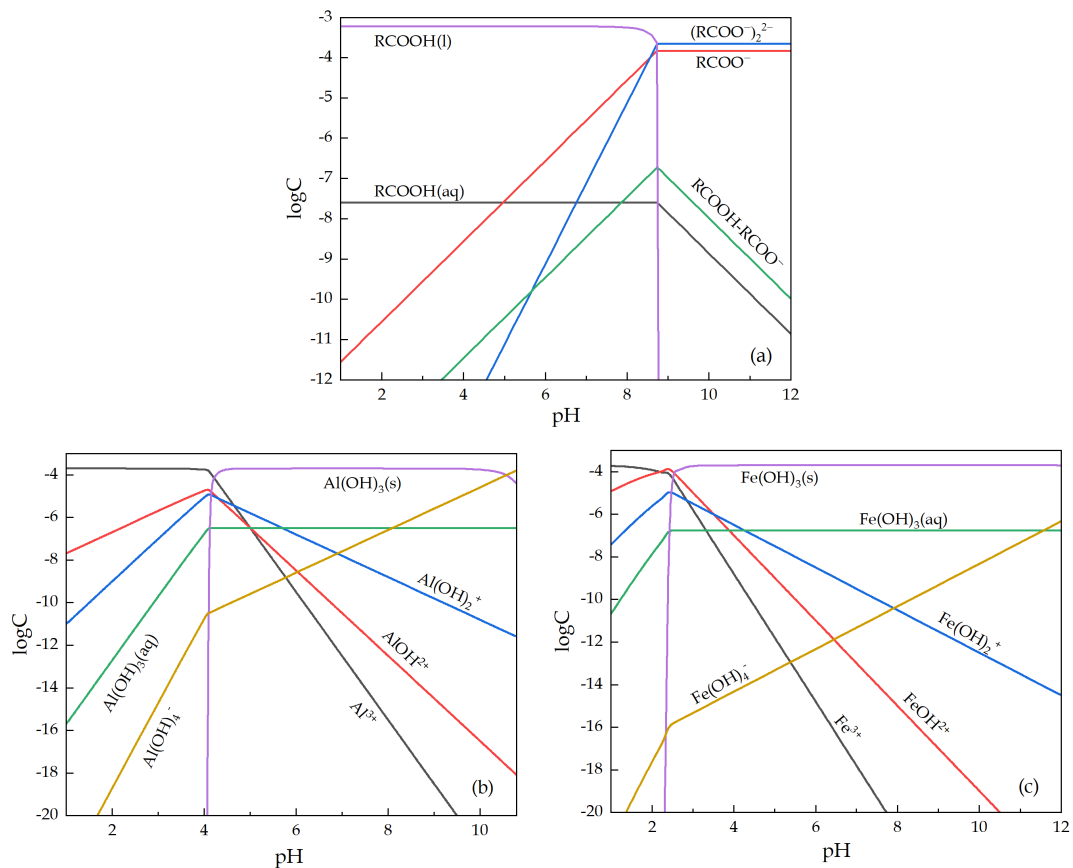


Fig. 4. Species distribution diagrams of NaOL (a), Al(III) (b) and Fe(III) (c) as a function of pH

conditions. By analyzing the equilibrium relationship within the solution, it is possible to determine the concentrations of these metal ion hydrolysis products at different pH levels. Computed diagrams depicting the hydrolysis components of Al^{3+} and Fe^{3+} with an initial concentration of 2×10^{-4} mol/L are provided in Fig. 4(b) and 4(c).

Consistent with the single mineral flotation test of K-feldspar, the activation of Al^{3+} and Fe^{3+} is most effective at a pH of approximately 9 and 10, respectively. These pH levels correspond to the primary components shown in the hydrolysis diagrams of Al^{3+} and Fe^{3+} , namely $\text{Al}(\text{OH})_3(\text{s})$ and $\text{Fe}(\text{OH})_3(\text{s})$. This observation suggests that aluminum hydroxide and iron hydroxide may significantly contribute to activating K-feldspar flotation. With the increase in pH, the concentrations of $\text{Al}(\text{OH})_4^-$ and $\text{Fe}(\text{OH})_4^-$ in the hydrolysis diagram exhibit a notable increase, leading to a substantial reduction in the flotation recovery rate of K-feldspar within this pH range. Hence, it can be inferred that $\text{Al}(\text{OH})_4^-$ and $\text{Fe}(\text{OH})_4^-$ exert an influence on the flotation process of K-feldspar.

3.3. Zeta-potential

Adsorption on mineral surfaces induces changes in surface charge, making zeta potential measurements an effective tool for understanding variations in mineral surface dynamics (Kim, Jinkeun, 2005). This method is employed to evaluate the influence of the presence or absence of metal ions on the mineral surface charge. As shown in Fig. 5, over the examined pH range of 4 to 11, the mineral surface potential remains negative, this finding is consistent with previously reported values for the surface potential of K-feldspar (Fuerstenau and Pradip, 2005).

The potential curve trajectory in the graph demonstrates that the introduction of NaOL shifts the surface potential of K-feldspar towards the negative charge direction. This shift corresponds to an increase in the concentration of fatty acid anions (RCOO^-), RCOO^- in the solution as the pH increases until it stabilizes. These observations highlight an interaction between NaOL and the K-feldspar surface. The relatively stable surface potential within the investigated pH range suggests a moderate NaOL adsorption on the feldspar surface, supporting the micro-flotation findings.

The introduction of Fe^{3+} into the suspension significantly increases the surface potential of untreated K-feldspar, transitioning from a positive to a negative surface charge as the pH rises. This finding suggests that Fe^{3+} can chemically adsorb onto the feldspar surface (Jie et al., 2014). Based on the preceding solution chemistry analysis, it is inferred that within the pH range of 4 to 8, the predominance of Fe^{3+} , $\text{Fe}(\text{OH})^{2+}$, and $\text{Fe}(\text{OH})_2^+$ maintains a stable positive surface charge, alongside the attachment of $\text{Fe}(\text{OH})_3$ precipitate. As pH exceeds 8, the concentration of $\text{Fe}(\text{OH})_4^-$ rises, and its adsorption onto the mineral surface results in a marked decrease in potential, turning negative (Peng et al., 2017). Additionally, the addition of Al^{3+} within a pH range of 4 to 10, owing to the presence of $\text{Al}(\text{OH})_2^+$ and the formation of $\text{Al}(\text{OH})_3$ precipitate, shifts the surface potential of K-feldspar towards the positive charge direction, keeping it stable. When pH surpasses 10, an ongoing hydroxylation reaction on the feldspar surface triggers a rapid shift from the surface's positive potential to negative (Xiao et al., 2022).

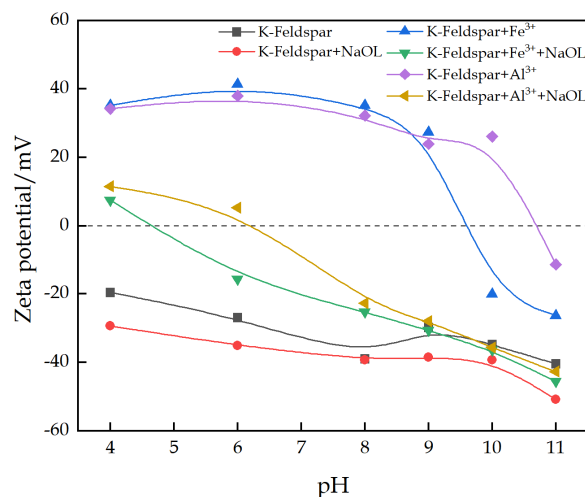


Fig. 5. Zeta potential of K-feldspar as a function of pH Formulae

The introduction of NaOL in the presence of metal ions induces a notable shift in the surface potential of K-feldspar towards the negative charge direction compared to its potential in the sole presence of metal ions. Furthermore, a distinct shift in the isoelectric point is observable. These results conclusively demonstrate the capacity of both Fe^{3+} and Al^{3+} to activate the K-feldspar surface, forming robust adsorption with NaOL.

3.4. FT-IR analysis

To investigate the effect of metal ions on K-feldspar flotation, the reaction products resulting from NaOL flotation, conducted at pH levels of 9 and 10 in the presence and absence of Fe^{3+} and Al^{3+} ions, were analyzed using FT-IR spectroscopy. The FT-IR spectra for the pure mineral K-feldspar and NaOL are presented in Fig. 6(a). A comparison of Fig. 6(b), in the presence of NaOL, reveals the emergence of subtle new absorption peaks at 2923 cm^{-1} and 2853 cm^{-1} . These peaks correspond to the asymmetric stretching vibrations of $-\text{CH}_3(-\text{CH}_2-)$ and the symmetric stretching vibrations of $-\text{CH}_2-$, respectively, indicating the adsorption of NaOL on the K-feldspar surface (Liu et al., 2015).

Several prominent peaks are detected in the $1200\text{--}400\text{ cm}^{-1}$ region of the K-feldspar's FT-IR spectrum (Fig. 6(c)). The peak at 1137.32 cm^{-1} corresponds to the Si-O stretching vibration, while the peak at 1009.56 cm^{-1} arises from the Si(Al)-O stretching vibration. Peaks at 769.73 cm^{-1} and 727.24 cm^{-1} represent the Si-Si and Si-Si(Al) stretching vibrations, respectively. Additionally, the O-Si(Al)-O bending vibrations correspond to peaks at 647.71 cm^{-1} and 581.14 cm^{-1} . The bending vibration of O-Si-O is indicated by the peak at 536.26 cm^{-1} , and the Si-O-Si bending vibration is associated with the peak at 417.99 cm^{-1} (Ishii et al., 1967).

As shown in Fig. 6(b), at a pH of 10, some characteristic peaks at 1137.32 cm^{-1} , 1009.56 cm^{-1} , 581.14 cm^{-1} , and 417.99 cm^{-1} exhibit various displacements due to the adsorption of NaOL. Notably, the peak at 581.14 cm^{-1} remains relatively stable with the introduction of Al^{3+} . In contrast, the peaks at 1137.32 cm^{-1} , 1009.56 cm^{-1} , and 417.99 cm^{-1} show more pronounced displacements upon the addition of Al^{3+} , with respective offset values of 0.69 cm^{-1} , -4.11 cm^{-1} , and -4.55 cm^{-1} . Additionally, an intriguing deviation emerges at 727.24 cm^{-1} , displaying an offset value of -1.47 cm^{-1} . Considering the relationship between characteristic peaks and vibration modes, the introduction of Al^{3+} appears to amplify the shifting of Si-O stretching vibration peaks towards longer wavelengths and encourages Si(Al)-O stretching, as well as Si-O-Si bending vibration peaks, to migrate towards shorter wavelengths. Simultaneously, it induces a shift of the Si-Si(Al) stretching vibration peak towards shorter wavelengths.

As depicted, at a pH of 9, the distinctive peaks at 1009.56 cm^{-1} , 769.73 cm^{-1} , 727.24 cm^{-1} , 536.26 cm^{-1} , and 417.99 cm^{-1} demonstrated significant shifts due to the adsorptive effect of the collector. The introduction of Fe^{3+} intensified the displacement of peaks at 1009.56 cm^{-1} and 727.73 cm^{-1} , while the peaks at 769.73 cm^{-1} , 536.26 cm^{-1} , and 417.99 cm^{-1} displayed a moderated shift, with deviations of -3.32 cm^{-1} , -2.68 cm^{-1} , 0.37 cm^{-1} , -0.87 cm^{-1} , and -0.47 cm^{-1} , respectively. These alterations indicate that the coordinated interaction of Fe^{3+} with NaOL may prompt a trend of migration towards longer wavelengths for Si-Si stretching vibration peaks, while simultaneously propelling the Si(Al)-O stretching, Si-Si(Al) stretching, O-Si-O bending, and Si-O-Si bending vibration peaks towards shorter wavelengths (Peng et al., 2017). The above analysis confirms that the presence of Al^{3+} and Fe^{3+} in the NaOL flotation of K-feldspar has a more pronounced impact on the surface characteristics of mineral.

3.5. XPS analysis

To gain a more comprehensive understanding of the mechanism of Al^{3+} and Fe^{3+} activation in the flotation of K-feldspar, XPS was applied to analyze the changes in surface chemical composition before and after ion treatment. Through an assessment of the full-spectrum scanning results under various treatment conditions (Fig. 7), the relative content of elements on the mineral surface was determined. Furthermore, to counter the surface charging effect, all binding energies were calibrated to the C1s spectrum at 284.8 eV .

Table 2 shows a 3.06 percentage points increase in the relative concentration of aluminum on the K-feldspar surface following the treatment with Al^{3+} and Fe^{3+} . Similarly, a corresponding 2.2 percentage points increase is observed in the relative concentration of iron, indicating the adsorption of both Al^{3+} and Fe^{3+} on the surface of K-feldspar. Notably, there is a significant rise in the relative concentration of

carbon on the surface during metal ion treatment (along with NaOL addition) compared to untreated K-feldspar, indicating the strong adsorptive capability of NaOL on the K-feldspar surface. Simultaneously, the concentrations of Al^{3+} and Fe^{3+} on the K-feldspar surface show respective declines of 3.75 and 1.5 percentage points, likely due to the interaction between aluminum and iron atoms and NaOL (Gong et al., 2020).

To gain a more comprehensive understanding of the activation mechanism, the fitting of high-resolution spectra of O1s, Al2p, and Fe2p from various samples was performed. As illustrated in Fig. 8, the binding energies associated with O element connections with Si and metal elements on the untreated K-feldspar surface were measured at 532.32 eV and 531.68 eV, respectively (Hagan, 1982). Following separate treatments with Al^{3+} and Fe^{3+} , the binding energies exhibited negligible changes. However, there was a notable shift in the relative distribution of O(II) between Si-O and hydroxy complexes, with the latter displaying an increase in both scenarios. This alteration may stem from the extensive adsorption of metal ion complexes on the mineral surface. Conversely, simultaneous treatment with metal ions and NaOL resulted in a reduction in the distribution of O(II) in the hydroxy complexes compared to independent metal ion treatments. This change could be attributed to a coordination reaction between surface metal ion hydroxy complexes and oleate ions (Han et al., 2021).

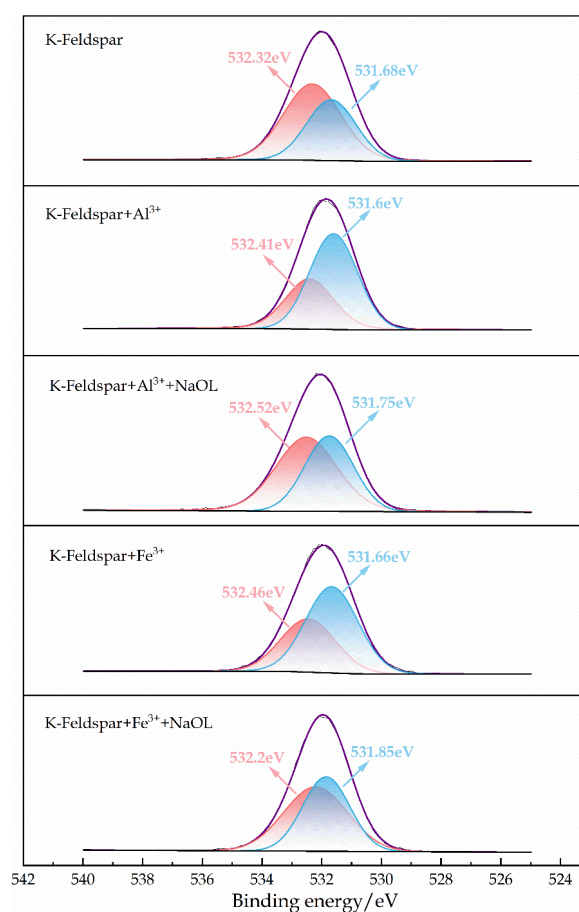


Fig. 8. O1s high-resolution spectra of K-feldspar surface under different conditions

As shown in Fig. 9, pristine K-feldspar exhibits a single peak at 74.46 eV, which corresponds to Al-O in aluminosilicate minerals. Following treatment with Al^{3+} , a new peak emerges at 74.14 eV on the K-feldspar, indicating Al-OH. The binding energy of Al-O shifts by 0.19 eV, suggesting a chemical interaction with Al^{3+} and K-feldspar (Luo et al., 2022; Luo and Chen, 2022). Upon the addition of NaOL, the binding energy of Al-O undergoes a significant shift, reaching 0.6 eV, while the binding energy of Al-OH remains relatively stable. This phenomenon can be attributed to the reaction of the aluminum hydroxyl complex with NaOL, forming an oleate complex and establishing a stable chemical bond (Xiao et al., 2022; Zhang et al., 2023; Eskanolou et al., 2022). Simultaneously, the aluminum hydroxide precipitate adsorbs onto the mineral surface, enhancing its hydrophobicity.

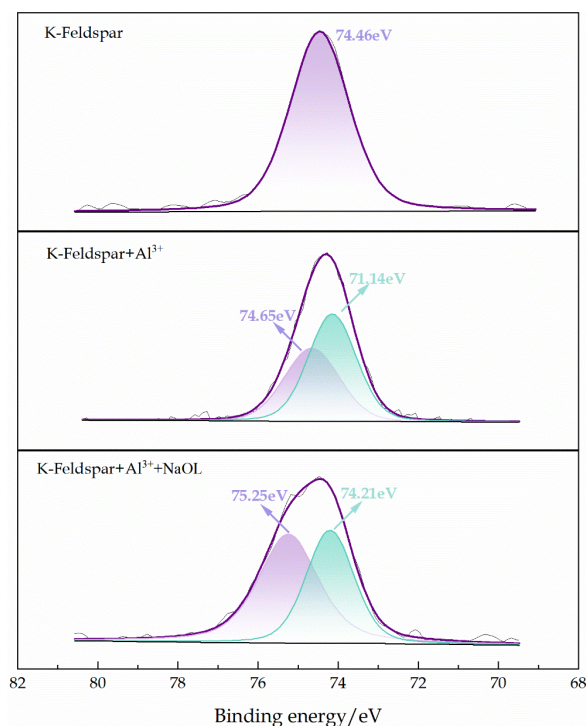


Fig. 9. Al₂p high-resolution spectra of K-feldspar surface under different conditions

A noticeable new peak appears in the K-feldspar spectra after Fe³⁺ treatment (Fig. 7). The Fe₂p spectra were fitted using a 2p_{1/2} and 2p_{3/2} doublet. The high-resolution XPS spectra of the Fe₂p_{3/2} peak (Fig. 10) exhibit two primary peaks at 724.69 eV and 711.09 eV, along with two satellite peaks. The peak at 711.09 eV is attributed to Fe³⁺ in Fe(OH)₃ (Biesinger et al., 2011; Carver et al., 1972). With the addition of NaOL, the Fe₂p_{3/2} peak shifts to 710.24 eV, indicating a coordination reaction between the oleate anion (RCOO⁻) in NaOL and Fe³⁺ ions. This coordination reaction occurs as the carboxyl group (-COO⁻) in the oleate anion forms a complex with Fe³⁺ ions, where electrons from the oleate anion partially transition to the electron orbitals of the Fe³⁺ ions, populating the energy levels of the Fe³⁺ ions (Chen, 2021; Tian et al., 2018). This implies that Fe³⁺ can act as a bridge, facilitating stable chemical adsorption between K-feldspar and NaOL.

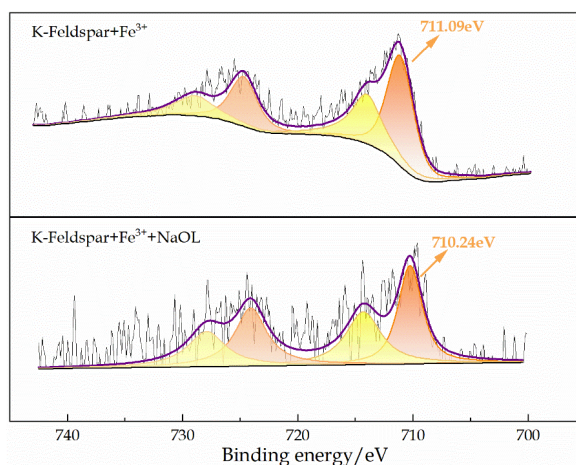


Fig. 10. Fe₂p high-resolution spectra of the surface of K-feldspar without NaOL in the presence of Fe(III)

3.6. Adsorption modeling and discussion

Based on FT-IR and XPS analyses, along with reference to previous research, adsorption models of Al(III) and Fe(III) ions activating K-feldspar flotation have been established. As shown in Fig. 11, there are two equilibrium systems centered around Si and Al on the feldspar surface: Si-O and Al-O bonds.

Comparatively, research has shown that Al-O bonds exhibit higher ionic characteristics, are weaker, more susceptible to breakage, and consequently more reactive, serving as the primary chemically adsorptive sites (Sun et al., 2023). Hydroxyl complexes adsorbed on mineral surfaces are formed by metal ions bonded to an oxygen atom on the mineral surface. Hydroxide precipitates adsorbed on mineral surfaces are formed by two oxygen atoms on the surface bonded to metal ions (chelation). Combined with previous infrared spectroscopic analysis did not indicate characteristic peaks related to -COO^- , suggesting that NaOL can coordinate with metal hydroxyl complexes and hydroxide precipitates through weak bonds, specifically: the negative charge of -COO^- in NaOL interacts electrostatically with the positive charge of metal ions to form ionic bonds. Simultaneously, the oxygen atoms in -COO^- can also interact with metal ions through van der Waals forces, ultimately forming stable complexes that facilitate more stable chemical adsorption, thereby enhancing the floatability of K-feldspar.

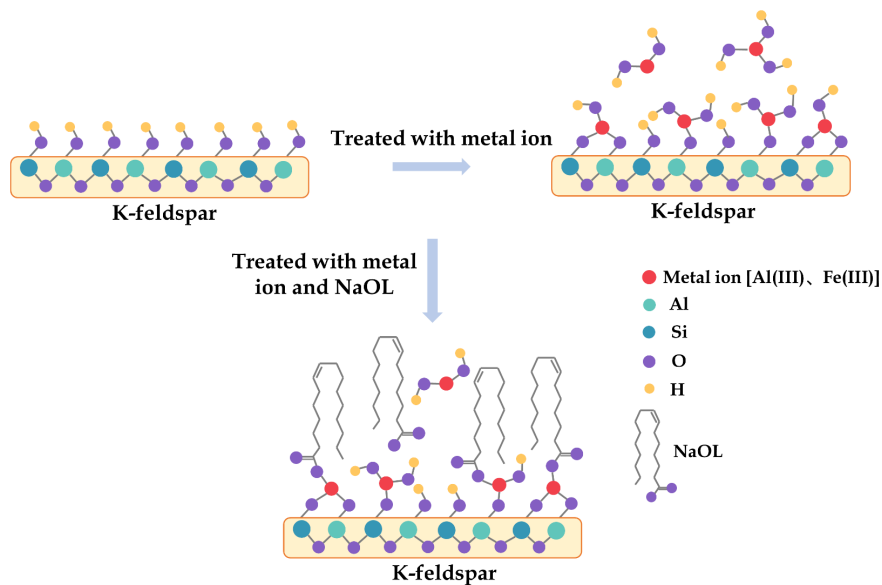


Fig. 11. Adsorption model of Al(III) and Fe(III) activated K-feldspar

4. Conclusions

The adsorption capacity of NaOL on the surface of K-feldspar is significantly enhanced by the presence of Fe(III) and Al(III) ions in the flotation system, resulting in an improved recovery rate of K-feldspar. The mechanism of this enhancement is that Fe(III) and Al(III) ions modify the surface potential and the bonding properties of K-feldspar surface atoms. These metal ions form metal hydroxyl complexes that are adsorbed on the surface. Meanwhile, NaOL dissociated into oleate ions (RCOO^-) and hydroxyl complexes that coordinate with the metal ions, forming hydrophobic complexes that attach to the K-feldspar surface. This process significantly facilitates the efficient collection of K-feldspar by NaOL. Therefore, the effects of Fe(III) and Al(III) ions on NaOL flotation of K-feldspar are significant, as they not only improve the flotation efficiency, but also alter the electrochemical properties of K-feldspar surface, these findings have great scientific significance for understanding and optimizing the role of metal ions in flotation process.

Acknowledgments

This research is supported by GDAS' Project of Science and Technology Development (2022GDASZH-2022010104, 2023GDASZH-2023010104), and the contributions of all members of the laboratory.

References

- BIESINGER, M.C., PAYNE, B.P., GROSVENOR, A.P., LAU, L.W.M., GERSON, A.R., SMART, R.ST.C., 2011. *Resolving surface chemical states in XPS analysis of first row transition metals, oxides and hydroxides: Cr, Mn, Fe, Co and Ni*. Appl. Surf. Sci. 257, 2717-2730.

- CARVER, J.C., SCHWEITZER, G.K., CARLSON, T.A., 1972. *Use of X-Ray Photoelectron Spectroscopy to Study Bonding in Cr, Mn, Fe, and Co Compounds*. J. Chem. Phys. 57, 973-982.
- CHEN, J., 2021. *The interaction of flotation reagents with metal ions in mineral surfaces: A perspective from coordination chemistry*. Miner. Eng. 171, 107067.
- CHEN, P., ZHAI, J., SUN, W., HU, Y., YIN, Z., 2017. *The activation mechanism of lead ions in the flotation of ilmenite using sodium oleate as a collector*. Miner. Eng. 111, 100-107.
- DEMIR, C., BENTLI, I., GÜLGÖNÜL, I., ÇELİK, M.S., 2003. *Effects of bivalent salts on the flotation separation of Na-feldspar from K-feldspar*. Miner. Eng. 16, 551-554.
- DEMIR, C., KARAGÜZEL, C., GÜLGÖNÜL, I., ÇELİK, M.S., 2004. *Selective Separation of Sodium and Potassium Feldspar Minerals from Orebodies*. Key Eng. Mater. 264-268, 1435-1438.
- ESKANLOU, A., HUANG, Q., FOUCAUD, Y., BADAWI, M., ROMERO, A.H., 2022. *Effect of Al³⁺ and Mg²⁺ on the flotation of fluorapatite using fatty- and hydroxamic-acid collectors - A multiscale investigation*. Appl. Surf. Sci. 572, 151499.
- FENG, Q., WEN, S., ZHAO, W., CHEN, Y., 2018. *Effect of calcium ions on adsorption of sodium oleate onto cassiterite and quartz surfaces and implications for their flotation separation*. Sep. Purif. Technol. 200, 300-306.
- FUERSTENAU, D.W., PRADIP, 2005. *Zeta potentials in the flotation of oxide and silicate minerals*. Adv. Colloid Interface Sci. 114-115, 9-26.
- GAIED, M.E., GALLALA, W., 2015. *Beneficiation of feldspar ore for application in the ceramic industry: Influence of composition on the physical characteristics*. Arab. J. Chem. 8, 186-190.
- GAO, Z., JIANG, Z., SUN, W., GAO, Y., 2021. *Typical roles of metal ions in mineral flotation: A review*. Trans. Nonferrous Met. Soc. China 31, 2081-2101.
- GONG, G., WANG, P., LIU, J., HAN, Y., ZHU, Y., 2020. *Effect and mechanism of Cu(II) on flotation separation of cassiterite from fluorite*. Sep. Purif. Technol. 238, 116401.
- Gülsoy, F.Ş.K., Ö.Y., n.d., 2000. *The effects of metal ions on the selectivity of feldspar-quartz separation*. Mineral Processing on the Verge of the 21st Century 21
- HAGAN, R.C., 1982. *X-ray fluorescence analysis major elements in silicate minerals* (No. LA-9400-MS, 6642056).
- HAN, G., WEN, S., WANG, H., FENG, Q., 2021. *Effect of ferric ion on cuprite surface properties and sulfidization flotation*. Sep. Purif. Technol. 278, 119573.
- HEYES, G.W., ALLAN, G.C., BRUCKARD, W.J., SPARROW, G.J., 2012. *Review of flotation of feldspar*. Miner. Process. Extr. Metall. 121, 72-78.
- ISHII, M., SHIMANOUCI, T., NAKAHIRA, M., 1967. *Far infra-red absorption spectra of layer silicates*. Inorganica Chim. Acta 1, 387-392.
- JIE, Z., WEIQING, W., JING, L., YANG, H., QIMING, F., HONG, Z., 2014. *Fe(III) as an activator for the flotation of spodumene, albite, and quartz minerals*. Miner. Eng. 61, 16-22.
- KIM, JINKEUN, 2005. *Characteristics of Zeta Potential Distribution in Silica Particles*. Bull. Korean Chem. Soc. 26, 1083-1089.
- KUANG, J.Z., YANG, Y., ZOU, Z., YUAN, W., HUANG, Z., CHENG, H., 2022. *Effect of metal ions on the dispersion and agglomeration behavior of micro-fine wolframite*. Colloids Surf. Physicochem. Eng. Asp. 643, 128747.
- LIU, W., ZHANG, S., WANG, W., ZHANG, J., YAN, W., DENG, J., FENG, Q., HUANG, Y., 2015. *The effects of Ca(II) and Mg(II) ions on the flotation of spodumene using NaOL*. Miner. Eng. 79, 40-46.
- LUO, A., CHEN, J., 2022. *Effect of hydration and hydroxylation on the adsorption of metal ions on quartz surfaces: DFT study*. Appl. Surf. Sci. 595, 153553.
- LUO, X.-P., ZHANG, Y.-B., ZHOU, H.-P., XIE, F.-X., YANG, Z.-Z., ZHANG, B.-Y., LUO, C.-G., 2022. *Flotation separation of spodumene and albite with activation of calcium ion hydrolysate components*. Rare Met. 41, 3919-3931.
- PENG, H., LUO, W., WU, D., BIE, X., SHAO, H., JIAO, W., LIU, Y., 2017. *Study on the Effect of Fe³⁺ on Zircon Flotation Separation from Cassiterite Using Sodium Oleate as Collector*. Minerals 7, 108.
- SANZ, J., TOMASA, O., JIMENEZ-FRANCO, A., SIDKI-RIUS, N., 2022. *Feldspar, in: Elements and Mineral Resources, Springer Textbooks in Earth Sciences, Geography and Environment*. Springer International Publishing, Cham, pp. 351-353.
- SONG, C., ZHOU, Y., LIU, Q., DENG, J., LI, S., GAO, L., YU, L., 2018. *Effects of BaCl₂ on K-feldspar flotation using dodecyl amine chloride under natural pH*. Trans. Nonferrous Met. Soc. China 28, 2335-2341.
- SUN, N., WANG, G., GE, P., SUN, W., XU, L., TANG, H., WANG, L., 2023. *Selective flotation of quartz from feldspar using hydroxypropyl starch as depressant*. Miner. Eng. 195, 108022.

- TIAN, M., LIU, R., GAO, Z., CHEN, P., HAN, H., WANG, L., ZHANG, C., SUN, W., HU, Y., 2018. *Activation mechanism of Fe (III) ions in cassiterite flotation with benzohydroxamic acid collector*. Miner. Eng. 119, 31-37.
- WANG, Z., WU, H., XU, Y., SHU, K., FANG, S., XU, L., 2020. *The effect of dissolved calcite species on the flotation of bastnaesite using sodium oleate*. Miner. Eng. 145, 106095.
- XIAO, W., SHAO, Y., YU, J., ZHANG, B., SHU, H., ZHANG, Y., 2022. *Activation of ilmenite flotation by Al³⁺ in the benzohydroxamic acid (BHA) system*. Sep. Purif. Technol. 299, 121770.
- XU, L., TIAN, J., WU, H., DENG, W., YANG, Y., SUN, W., GAO, Z., HU, Y., 2017. *New insights into the oleate flotation response of feldspar particles of different sizes: Anisotropic adsorption model*. J. Colloid Interface Sci. 505, 500-508.
- XU, L., TIAN, J., WU, H., FANG, S., LU, Z., MA, C., SUN, W., HU, Y., 2018. *Anisotropic surface chemistry properties and adsorption behavior of silicate mineral crystals*. Adv. Colloid Interface Sci. 256, 340-351.
- YANG, Y., MIN, Y., LOCOCO, J., JUN, Y.-S., 2014. *Effects of Al/Si ordering on feldspar dissolution: Part I. Crystallographic control on the stoichiometry of dissolution reaction*. Geochim. Cosmochim. Acta 126, 574-594.
- ZENG, W., ZHANG, G., SHI, Q., OU, L., 2022. *Effects and Mechanism of Fe³⁺ on Flotation Separation of Feldspar and Epidote with Sodium Oleate at Natural pH*. Separations 9, 110.
- ZHANG, X., REN, L., ZHANG, Y., BAO, S., 2023. *Effect of aluminum ion on rutile flotation*. Miner. Eng. 198, 108083.
- ZHANG, Y., HU, Y., SUN, N., LIU, R., WANG, Z., WANG, L., SUN, W., 2018. *Systematic review of feldspar beneficiation and its comprehensive application*. Miner. Eng. 128, 141-152.
- ZHOU, Y., HU, Y., WANG, Y., 2011. *Effect of metallic ions on dispersibility of fine diasporite*. Trans. Nonferrous Met. Soc. China 21, 1166-1171.